

A Policy Adaptation Method for Implicit Multitask Reinforcement Learning Problems

Satoshi Yamamori and Jun Morimoto

Abstract—In dynamic motion generation tasks, including contact and collisions, small changes in policy parameters can lead to extremely different returns. For example, in soccer, the ball can fly in completely different directions with a similar heading motion by slightly changing the hitting position or the force applied to the ball or when the friction of the ball varies. However, it is difficult to imagine that completely different skills are needed for heading a ball in different directions. In this study, we proposed a multitask reinforcement learning algorithm for adapting a policy to implicit changes in goals or environments in a single motion category with different reward functions or physical parameters of the environment. We evaluated the proposed method on the ball heading task using a monopod robot model. The results showed that the proposed method can adapt to implicit changes in the goal positions or the coefficients of restitution of the ball, whereas the standard domain randomization approach cannot cope with different task settings.

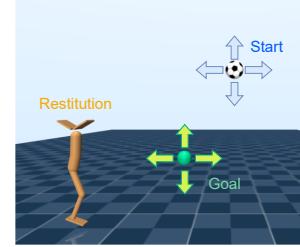
Index Terms—Robot learning; Meta reinforcement learning; Transfer learning; Manipulation; Policy selection

I. INTRODUCTION

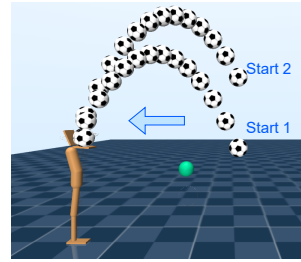
MULTITASK reinforcement learning (multitask RL) has been gaining attention as a promising tool to develop human-level skillful agents. In particular, the meta-reinforcement learning (meta-RL) approach that updates shared policy parameters among different policies for different tasks has become a major research topic for optimizing the parameters of the policies to cope with the multitask RL problems [1]–[4]. However, most meta-RL approaches train multiple policy networks for each task. Therefore, several policy networks must be trained to acquire a policy set to manage several tasks. In football, for example, the ball can fly in completely different directions with a similar heading motion by slightly changing the hitting position, the force applied to the ball, or when the friction of the ball is different. In such cases, continuous task changes may have infinite numbers of task goals, and preparing policy networks for all these tasks becomes impossible.

Therefore, in this study, we propose a training procedure for policies represented by deep neural networks to cope with the multitask RL problems with implicit task changes. We were particularly interested in the task change within the same movement category, that is, heading a ball to different goal locations. As the concrete learning framework, we developed a novel adaptation method for the contextual Markov decision process (cMDP) to cope with the implicit multitask problems

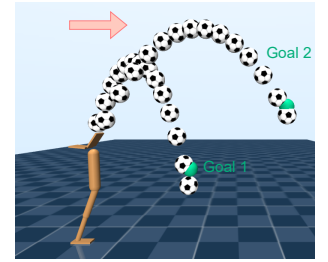
Satoshi Yamamori and Jun Morimoto are with the Department of Brain Robot Interface, ATR Computational Neuroscience Laboratories, Kyoto, 619-0288, Japan (E-mail: yamamori@atr.jp, xmorimo@atr.jp), and also with the Graduate School of Informatics, Kyoto University.



(a) Multitask heading



(b) Throw in



(c) Hitting ball

Fig. 1. Multitask heading problem. Monopod robot model tries to acquire policies to hit the ball back to multiple goals in multiple environments.

based on the idea of a variational inference framework [3]. We demonstrated that selecting a base network model according to the learning performance with randomized task parameters is the key to successful adaptation to multiple reward and environmental settings. Furthermore, our proposed method simultaneously acquires the optimal policy for each context and encoder to embed context variables that correspond to the task settings. The context-related latent variable was estimated to adapt the policy to the novel tasks, that is, unknown reward and environmental settings. We showed that the Bayesian optimization method can be efficiently used to update the latent variable in the adaptation procedure in cases where the task-relevant variable space is low dimensional.

We evaluated our proposed policy adaptation method using the monopod motor control task (See Fig. 1). In this task, the monopod model tries to hit the ball back to the target point while maintaining the posture until hitting the ball. To show the adaptation performance of the proposed method, the target points as well as the coefficient of restitution that defines the physical interaction between the ball and the monopod model were changed. We demonstrated that the monopod model was successfully adapted to the implicitly changing task settings. The contributions of our study can be summarized as follows:

- We developed a policy adaptation method that can cope with implicit multitask problems. The proposed method is composed of three phases: 1) policy generation, 2) policy selection, and 3) policy adaptation.
- We demonstrated that selecting the base policy from policy pool derived in the policy generation phase in terms of learning performance is the key to successful adaptation.
- We showed that the monopod model was able to hit the ball back to novel target points with different physical interaction settings using the proposed policy adaptation method.

The remainder of this paper is organized as follows: In section II, we described the related studies. In section III, we introduced the proposed adaptation method. In section IV, we explained the experimental settings for the monopod model used for evaluating the proposed method. In section V, we presented the results. In section VI, we discussed the comparison of the proposed method with the standard approach as well as the limitations of the proposed method. Finally, in Section VII, we presented the conclusions of the study.

II. RELATED WORKS

A. Goal-conditioned RL

To acquire a policy that can cope with multiple task goals, goal-conditioned RL methods have been developed [5]–[9]. By acquiring a goal-conditioned value function, the learned policy can generate optimized behaviors according to the continuously changing task goals [6], [10], and [11]. Moreover, some studies proposed to use an image as a task goal [7], [10]. However, this approach essentially just selects a policy corresponding to a specified task goal and cannot handle implicitly changing task goals. In this study, we propose a three-phase learning and adaptation procedure to cope with the implicitly changing environmental settings and task goals.

B. Data-driven System Identification

To cope with a novel environment by an online data-driven approach, adaptive control methods have been widely studied [12]. If we cannot rely on a parametric environmental model which is usually built based on domain-specific knowledge, we can use an approximated model possibly represented by a neural network to bridge the gap between the current estimated and the actual environmental settings. Our early studies proposed collecting data by first using a robust policy that can deal with the novel environment and further improving the policy based on the approximated physical model by using the newly acquired data from the novel environment [13], [14]. Recently, instead of using the robust policy, acquiring a policy network that takes physical parameters as inputs has been proposed [15]. The environment-aware policy was acquired under a variety of environmental settings in the training phase, and in the test phase, the physical parameters were identified to further improve the performance of the policy. This approach has been further explored by using a low-dimensional representation of the physical parameters. In the training phase, the low-dimensional latent parameter space

was extracted. Then, in the test phase, the latent parameters were identified through interaction with the novel environment. The above approach was adopted to deal with the simulation-to-real gap [4], [16]. In this study, we applied these system identification approaches to the implicit multitask RL problem. We showed that the policies can be adapted not only to novel environments but also to novel tasks.

C. Policy Selection

In this study, we proposed an approach to find an adaptable base policy to unknown tasks and environments. To detect the adaptable policy, we must consider the policy selection problem [17]. Our proposed method selected the adaptable base policy by evaluating the learning performances of each policy generated in the policy generation phase.

D. Derivative-free Optimization

For solving optimization problems that have many low-quality local minima, using a gradient-based optimization method is not suitable. In such cases, using a derivative-free approach such as the evolution strategy can be useful. Furthermore, the evolution strategy has been explored for solving optimization problems [18], [19]. In the adaptation phase of our proposed method, we adopted the derivative-free RL approach to avoid low-quality local minima in the context-related variable space extracted by the acquired encoder network. As the derivative-free optimization method, we used the tree-structured Parzen estimator (TPE) [20], [21] that is well known as the high-performance parameter optimization method. In general, derivative-free methods do not work well in high-dimensional optimization problems. However, since the context-related variable space extracted in the adaptation phase was low-dimensional, our proposed method performed well with the derivative-free optimization method.

III. METHOD

In this section, we first defined the cMDP to formulate multitask reinforcement learning where the task goal or environments change implicitly. We then introduced the novel variational inference-based reinforcement learning method to cope with the cMDP.

A. Solving MDP through KL-divergence minimization

Here, we considered a cumulative reward to search for the optimal policy in the maximum entropy RL framework as follows:

$$\max_{\pi} \mathbb{E}_{\tau|\pi} \left[\sum_{t=0}^T (r(s_t, a_t) - \alpha \log \pi(a_t|s_t)) \right], \quad (1)$$

where $\tau = \{s_0, a_0, \dots, s_t, a_t, \dots, s_T, a_T\}$ is the state and action trajectory; $r(s_t, a_t)$ is the reward function; $\pi(a_t|s_t)$ is the policy; and the hyperparameter $\alpha \geq 0$ regulates the trade-off between exploration and exploitation [22]. It is known that the entropy-regularized RL problem can be reformulated as the inference problem of the policy distribution, where policy distribution is derived by minimizing the KL divergence

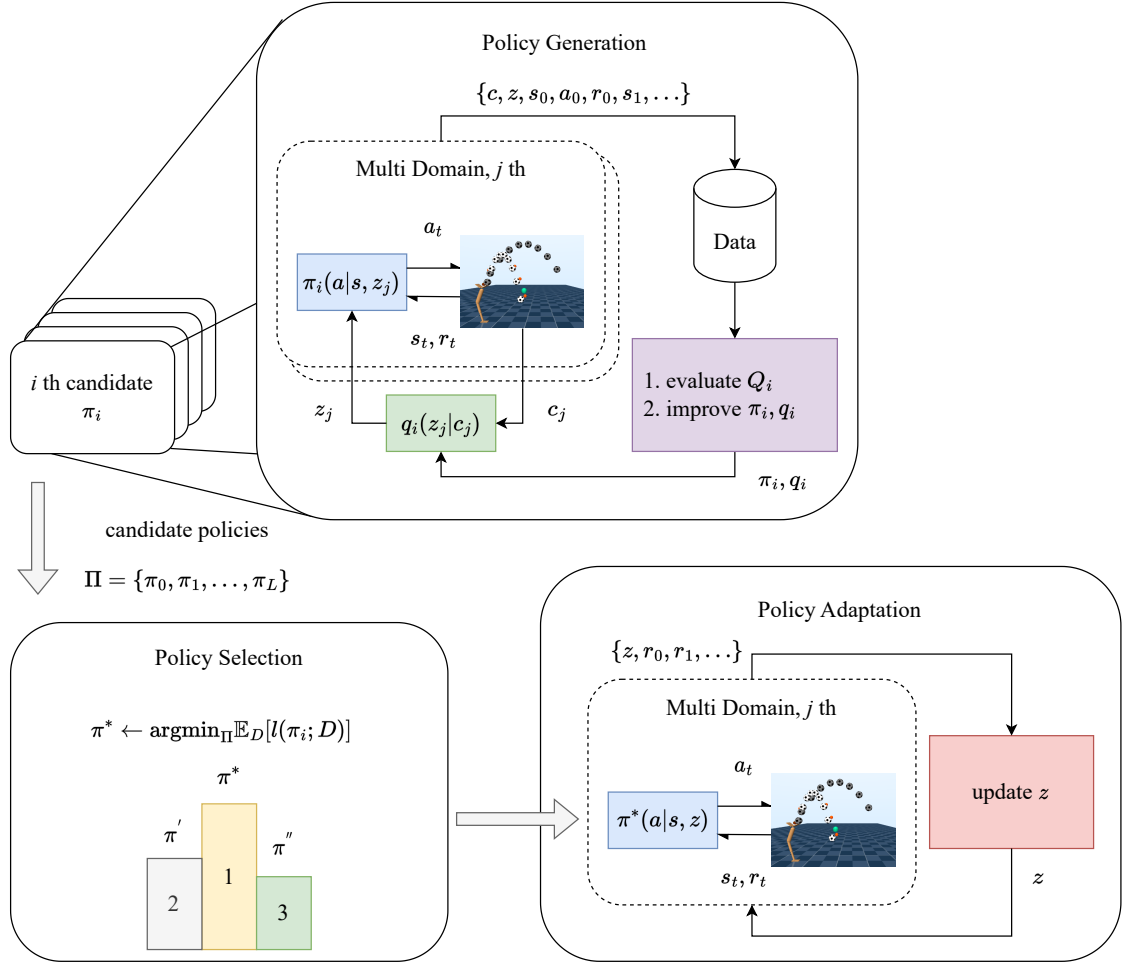


Fig. 2. Proposed three-phase multitask learning method. The proposed method is composed of three phases: generation, selection, and adaptation phases. In the policy generation phase, multiple candidate policies are generated under multiple domains. (a) The i -th candidate policy π_i is trained under the j -th domain. In the policy selection phase, one policy is selected from the candidate policy set for the adaptation phase. (b) The policy selection phase chooses a policy based on the statistical distance from L candidate policies. In the policy adaptation phase, low-dimensional latent variables are optimized for adapting to novel tasks and environments. (c) The latent variable z is optimized based on the task performance of the new domain.

between the distributions of the trajectory generated by the policy as,

$$q(\tau) = \prod_{t=0}^T q(s_{t+1}|s_t, a_t) \pi(a_t|s_t), \quad (2)$$

and the trajectory distribution induced by the reward as,

$$p(\tau) = \prod_{t=0}^T p(s_{t+1}|s_t, a_t) \exp(r(s_t, a_t)/\alpha). \quad (3)$$

We then found that minimizing the KL divergence leads to the maximization of the entropy-regularized cumulative reward as follows:

$$\begin{aligned} \alpha \text{KL}[q|p] &= \alpha \mathbb{E}_q[\log q - \log p] \\ &= \mathbb{E}_q \left[\sum_{t=0}^T \alpha \log \pi_t - r_t \right]. \end{aligned} \quad (4)$$

Notably, we can regard the above approach as discounted cumulative reward optimization by simply considering modified dynamics $\bar{p}(s_{t+1}|s_t, a_t) = \gamma p(s_{t+1}|s_t, a_t)$. In this case,

transition with $1 - \gamma$ into an absorbing state with zero rewards no matter what actions were taken [23].

B. Solving cMDP

In this subsection, we introduced the proposed variational inference-based RL method for solving the contextual MDP. A cMDP $\{\mathcal{A}, \mathcal{S}, \mathcal{C}, r, p, p_0\}$ has the state space \mathcal{S} , action space \mathcal{A} , context space \mathcal{C} , reward function $r(s, a, c) \in \mathbb{R}$, state transition probability $p(s'|s, a, c) \in \mathbb{R}$, and initial distribution of the state and context $p_0 = p(s_0)p(c) \in \mathbb{R}$. State transition probability and reward functions are conditioned with a vector c in context space \mathcal{C} . To acquire the optimal policy in cMDPs, we trained a policy $\pi(a|s, z)$ which depended not only on states s but also on the latent variable z . Here, the latent variable z is a context-relevant feature vector that is sampled from an encoder distribution $q(z|c)$. In other words, the encoder converts the current context variables c to the latent variable z .

In this study, we proposed a learning procedure to optimize

the policy and encoder for a cMDP.

$$\min_{\pi, q} \alpha \text{KL}[q|p] = \alpha \mathbb{E}_q [\log q - \log p], \quad (5)$$

$$q(\tau, z, c) = p(c)q(z|c) \prod_{t=0}^T p(s_{t+1}|s_t, a_t, c) \pi(a_t|s_t, z),$$

$$p(\tau, z, c) = p(c)\rho(z) \prod_{t=0}^T p(s_{t+1}|s_t, a_t, c) \exp(r(s_t, a_t, c)/\alpha).$$

The variational distribution q is the probability of trajectory τ under context $c \sim p(c)$ and latent variable $z \sim q(z|c)$. Likewise, a generative model p is the target distribution close to the variational distribution q ; $\rho(z)$ is the prior distribution; and α is the scale parameter. The variational distribution and generative model share the context distribution $p(c)$ and transition distribution $p(s_{t+1}|s_t, a_t, c)$. Therefore, cumulative rewards with entropy regularization by canceling out shared distribution were obtained as follows:

$$\begin{aligned} \alpha \text{KL}[q|p] &= \alpha \mathbb{E}_q [\log q - \log p] \\ &= \mathbb{E}_q \left[\alpha \log \frac{q(z|c)}{\rho(z)} + \sum_{t=0}^T \alpha \log \pi_t - r_t \right] + \text{const} \\ &\propto \mathbb{E}_{s_0, c} [\alpha \text{KL}[q(z|c)|\rho(z)] - V^\pi(s_0, c)], \end{aligned} \quad (6)$$

$$V^\pi(s, c) := \mathbb{E}_{\tau, z|s, c} \left[\sum_{t=0}^T r_t - \alpha \log \pi_t \right]. \quad (7)$$

In the policy evaluation step, the value function was computed by solving the soft bellman equation as follows:

$$Q^\pi(s, a, c) := r(s, a, c) + \mathbb{E}_{p(s'|s, a, c)} [V^\pi(s', c)], \quad (8)$$

$$V^\pi(s, c) = \mathbb{E}_{q(z|c)\pi(a|s, z)} [Q^\pi - \alpha \log \pi]. \quad (9)$$

In the policy improvement step, the policy and encoder were updated to minimize the KL divergence as,

$$\min_{q, \pi} \mathbb{E}_{s, c} [\beta \text{KL}[q(z|c)|\rho(z)] - V^\pi(s, c)]. \quad (10)$$

By comparing Eq. (6) with Eq. (10), the policy and encoder minimize the KL divergence between the variational distribution and the generative model.

C. Learning Algorithm

The proposed multitask learning algorithm is composed of three phases: generation, selection, and adaptation phases, as shown in Fig. 2.

1) *Generation Phase*: In the generation phase, the policy was trained under multiple contexts (see Algorithm 1). In the policy evaluation step, we first updated the approximated action value function Q_ϕ to empirically reduce the Bellman residual as follows:

$$\min_{\phi} \mathbb{E}_{\mathcal{D}} (Q(s, a, c; \phi) - r(s, a, c) - \gamma \bar{V}(s', c))^2. \quad (11)$$

We then updated the policy and the encoder using the KL divergence introduced in (10) as follows:

$$\max_{\psi, \eta} \mathbb{E}_{(s, c) \sim \mathcal{D}} [\bar{V}(s, c)] - \beta \mathbb{E}_{c \sim \mathcal{D}} \text{KL}[q|\rho], \quad (12)$$

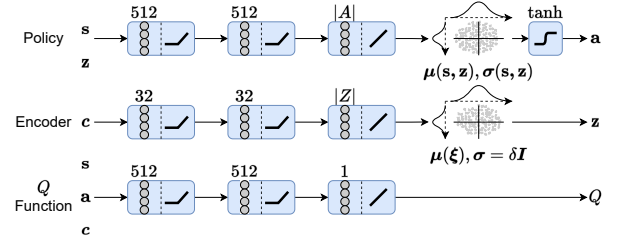


Fig. 3. Network Architecture. Our proposed method utilized three neural networks, namely, policy network, encoder network, and Q -network which approximate the action-value function. All networks contained two hidden layers, and the numbers on each block represent the layer size. Inputs to the policy network included state s and latent variable z . The encoder network considered the context variable c as the input. The Q -network received state s , action a , and context c as inputs.

where \mathcal{D} denotes the sample set in the replay buffer, and the state value function V can be derived as follows:

$$\begin{aligned} \bar{V}(s, c) &= Q(s, a', c; \phi) - \alpha \log \pi(a'|s, z'; \psi), \quad (13) \\ a' &\sim \pi(a|s, z'; \psi), \quad z' \sim q(z|c; \eta). \end{aligned}$$

ϕ , ψ , and η represent the parameters of the Q function, the policy, and the encoder, respectively. Fig. 3 shows the architecture of each network.

The prior of the latent variable $\rho(z)$ was derived by a standard multivariate normal distribution. The replay buffer stored the tuple $\{s, a, r, s', c\}$.

Algorithm 1 Generation Phase

- 1: **Input:** $\phi_{\{1,2\}}, \psi, \eta$
 - 2: $\phi_{\{1,2\}}^{\text{target}} \leftarrow \phi_{\{1,2\}}$
 - 3: $\mathcal{D} \leftarrow \emptyset$
 - 4: **for** each epoch **do**
 - 5: sample domain and encoded parameter:
 $z \sim q(z|c; \eta), c \sim p(c)$
 - 6: **for** collect state-action steps **do**
 - 7: $a_t \sim \pi(a|s, z; \psi)$
 - 8: $s_{t+1} \sim p(s_{t+1}|s_t, a_t, c)$
 - 9: $\mathcal{D} \leftarrow \mathcal{D} \cup \{(s_t, a_t, r(s_t, a_t, c), s_{t+1}, c)\}$
 - 10: **end for**
 - 11: **for** each gradient step **do**
 - 12: update policy ψ
 - 13: update encoder η
 - 14: update Q -function $\phi_{1,2}$
 - 15: update temperature α
 - 16: update target Q -function $\phi_{1,2}^{\text{target}}$
 - 17: **end for**
 - 18: **end for**
 - 19: **Output** $\phi_{\{1,2\}}, \psi, \eta$
-

2) *Selection*: One of the key ideas of our proposed method was to select a policy model based on the return values in the policy generation phase. As a well-known issue, the task performance of a policy highly depends on an exploration procedure determined by a random seed. Thus, in this paper, we proposed the generation of multiple policy models in the offline RL manner to find a high-quality policy that can adapt to a novel task from the generated policy models. The detailed

selection procedure is explained in Algorithm 2. The average reward over the k -th episode, l_k , was stored in the generated k -th policy model. We then selected the policy model based on the KL loss in Eq. (10) by substituting the value function with Eq. (7).

Algorithm 2 Selection Phase

- 1: Reset candidate policies $\Pi = \phi$
 - 2: Setup randomized domain with num_c contexts $\{c\}$
 - 3: **for** iteration $k = 1, \dots, K$ **do**
 - 4: Train π_k with contexts $\{c\} \triangleright$ Generation Phase
 - 5: Rollout π_k and collect $R(c) := \sum_t \gamma^t (r_t - \alpha \log \pi_t)$
 - 6: $l_k = \frac{1}{\text{num}_c} \sum_c \left[\beta \log \frac{q(z|c)}{\rho(z)} - R(c) \right]$ in Eq. (10)
 - 7: $\Pi \leftarrow \Pi \cup \{\pi_k, l_k\}$
 - 8: **end for**
 - 9: Select π_s based on sorted Π by $\{l_k\}$
 - 10: Deploy π_s to domain with new context c'
-

3) *Adaptation Phase*: The encoder network learns the latent variable space, where the context variables are embedded in this latent space. In the adaptation phase, we only optimized the latent variable such that the policy could cope with a novel domain.

To estimate the latent variable z based on the KL loss under the context c , we solve the following optimization problem:

$$z^* = \arg \max_z J(z),$$

$$J(z) = R(z) - \beta \text{KL}[P(*|z) \parallel \rho(*)], \quad (14)$$

$$R(z) = \sum_{t=0}^{T-1} \gamma^t (r_t - \alpha \log \pi_t(z)).$$

Adaptation Encoder $P(*|z)$ is represented with multivariate normalized distribution $\mathcal{N}(z, \mathbf{I})$. As we adopted a one-dimensional latent space, black-box optimization methods were utilized. As a concrete optimization method, we chose the TPE, which has been used as a standard tool for searching hyperparameters [20], because it shows empirically better optimization performance than other types of Bayesian optimization methods, such as the GPs and random search methods [20], [21]. To solve the optimization problem, TPE estimates the conditional distribution $p(z|J)$ from sampled data $\mathcal{D} = \{(z, J)\}$. We adopted the off-the-shelf implementation provided in the hyperparameter optimization framework, Optuna [24]. The mean z of encoder distribution is suggested by TPE for each iteration, as shown in Algorithm 3. The algorithm rollouts the policy based on the suggested latent variable z_k to collect the return value $J(z_k)$ and stores it in the replay buffer. The TPE updates the posterior distribution model for the next suggestion. The rollout will be iterated k_{\max} times. Finally, the algorithm returns the best value z^* stored in the replay buffer \mathcal{D} .

IV. EXPERIMENTS

We evaluated the proposed learning method using the monopod heading task, which is as shown in Fig. 1. Simulated experiments were conducted on the sagittal plane using

Algorithm 3 Adaptation Phase

- 1: $\pi \leftarrow$ trained policy in Policy Search phase
 - 2: $\mathcal{D} \leftarrow \emptyset$
 - 3: $z^* = \mathbf{0}$
 - 4: TPE model initialization
 - 5: **for** iteration $k = 1, \dots, k_{\max}$ **do**
 - 6: $z_k \leftarrow$ TPE suggests
 - 7: $J(z_k) \leftarrow$ Rollout policy $\pi(a|s, z_k)$ in Eq. (14)
 - 8: Store $(z_k, J(z_k))$ in \mathcal{D}
 - 9: TPE updates model $p(z|J)$
 - 10: **end for**
 - 11: Select z_k based on the sorted \mathcal{D} by indices J_k
-

a dynamics simulator MuJoCo [25]. Through this dynamic movement control task, we showed that the monopod robot model can adaptively accomplish multiple tasks in multiple environments using the proposed method.

A. Monopod heading task

In the monopod heading task, the robot model tried to hit a ball back to a specified goal point while maintaining the balance until hitting the ball. As small changes in the movement result in significantly different reward values, precise dynamic movement control is necessary. The reward function for the task is defined as follows:

$$r = \exp(-\lambda_1 \|p_{\text{ball}} - p_{\text{targ}}(t, c)\|^2) - \lambda_2 \|\tau\|^2, \quad (15)$$

where p_{ball} denotes the ball position; $p_{\text{targ}}(t, c)$ is the context-dependent desired ball trajectory; and τ denotes the joint torque vector. The desired ball trajectory was derived using the motion equation from a desired hit position to a target point within a given ball movement duration. The learning trial was terminated if the ball position deviated from the desired ball trajectory by a certain distance. The parameters of the reward were set to $\lambda_1 = 10.0$ and $\lambda_2 = 5.0 \times 10^{-3}$. Furthermore, we terminated the learning trial when the distance between the head position and the desired hitting position exceeded a certain threshold, primarily because the monopod robot fell to the ground.

The monopod robot model had five joints, and each joint was controlled by a proportional servo (P) controller. The state variables of the robot are listed in Table I. Notably, the goal position was not observed by the robot, although the task achievement was informed through the reward signal. The action variables were the target joint angles for the P controller at each joint.

In this task, five context variables were considered, which are presented in Table II. The coefficient of restitution defines a physical parameter of the ball and describes the relationship between the ball's velocities before and after hitting the ball. Horizontal and vertical goal position variables define different goal locations, and horizontal and vertical throw-in positions represent different ball throw positions toward the monopod robot.

TABLE I
OBSERVABLES

	Dimensionality	Type
Center of mass	2	float
Head position	2	float
Foot position	2	float
Joint angle	5	float
Joint angular velocity	5	float
Ball position	2	float
Ball velocity	2	float
One-step before action	5	float
Total dimensionality	25	

TABLE II
CONTEXT VARIABLES

	Type	Settings
Coefficient of restitution	float	{small, large}
Horizontal goal position	float	{near, far}
Vertical goal position	float	{low, high}
Horizontal throw-in position	float	{near, far}
Vertical throw-in position vertical-axis	float	{low, high}

B. Network models

The policy network was implemented using the multilayer neural network model. The network model had two hidden layers, shown in Fig. 3. The input variables to the network included the robot state s and the latent variable of the encoder z . The encoder network encoded the context variable c to the latent variable z and implemented a neural network model with two hidden layers. In the policy search phase, the encoder and Q-function networks were trained using actual context variables c . Subsequently, in the adaptation phase, the encoder network was not used. The latent variable z was estimated through adaptation trials.

C. Generating policy models

In the policy generation phase, we trained the networks under the combination of context variables. In other words, we conducted domain randomization with 32 different combinations of context variables as five context variables with two settings were considered, that is, $2^5 = 32$. We repeated this learning process 25 times to generate 25 different domain randomized policies with different random seeds.

D. Selecting a candidate policy network

Only one policy was selected from the 25 candidate policies using the policy selection method, as described in Algorithm 2.

E. Evaluating the adaptation performance

Herein, we evaluated how the monopod model can efficiently adapt to novel tasks and environments using our proposed method. The parameters representing the novel settings were uniformly sampled from intervals defined in Table II. Concretely, we randomly sampled 32 settings and fixed these values to evaluate the task performances of each method. We confirmed that these 32 settings were different from those used

in the policy generation phase described in Section IV-C. We then compared the proposed approach with the policy acquired using the domain randomization method, which is widely used to cope with an unknown environment.

F. Evaluating policy selection performance

We compared the proposed policy selection method with random selection in terms of top-one regret, which has been adopted to evaluate policy models [26]. The top-one regret evaluates the error between the best return value and the actual return. In this study, we compared the return value of the selected policy using the proposed method with that of the best policy that acquired the highest return among the candidate policies as follows:

$$\frac{1}{N} \sum_{i=1}^N |R_{\text{best}} - R_{\text{selected}}|, \quad (16)$$

where R_{best} denotes the return value of the best policy, and R_{selected} denotes that of the selected policy using the proposed method. To reliably evaluate the top-one regret, we used a bootstrap method. Concretely, as described in Section IV-C, we generated 25 candidate policies. Subsequently, we sampled five policies with replacements from the 25 candidates. Through the sampling procedure described above, we made 1000 sets of the five policies, that is, $N = 1000$.

V. RESULTS

A. Policy Adaptation Performance

To cope with multiple tasks and environments, domain randomization is one of the frequently used approaches. We first evaluated the acquired monopod heading policies using domain randomization as baseline. We trained the networks under the combination of context variables. The procedure to train the network was same as that described in Section IV-C. Notably, the proposed method also trained the encoder network in addition to the policy network while the domain randomization method did not.

Fig. 4 shows the monopod heading task performances at a novel goal position. As shown in the rightmost panel of Fig. 4(a), the ball deviated from the goal position when a policy acquired by domain randomization was adopted. Using the proposed method, the ball hit by the monopod successfully tracked the desired trajectory and passed around the goal position, as depicted in Fig. 4(b). Of note, the monopod model also learned to maintain its balance for hitting the ball.

Fig. 5 shows the task performances of the policies trained by the domain randomization (green bar) and the proposed adaptation (red bar). Each box plot was depicted based on 32 task performances, as described in Section IV-E. Both the domain randomization and generation phase of the proposed method trained the networks for 3×10^6 time steps, which approximately corresponds to 45,000 trials. The adaptation phase only required additional 100 trials to achieve successful performance in novel tasks.

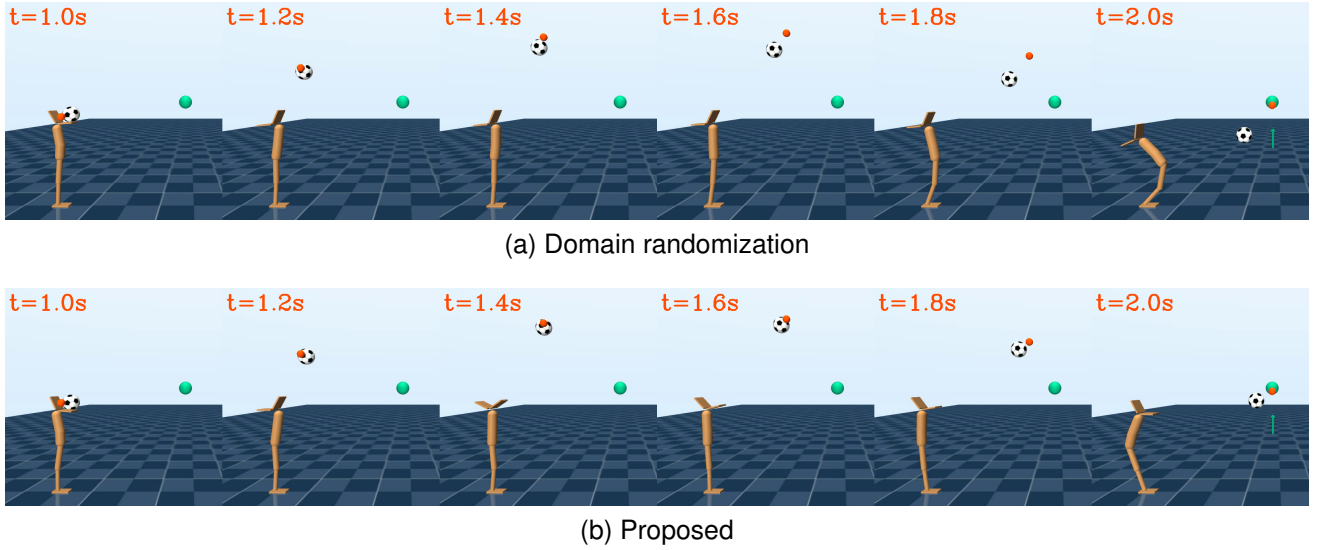


Fig. 4. Monopod heading performances with the novel goal position. The leftmost snapshot shows the timing of hitting the ball, that is, $t = 1.0$ s. The green sphere indicates the goal position. The red dot indicates the desired trajectory. (a) Heading performance by domain randomization. As shown in the rightmost panel, at $t = 2.0$ s, the ball deviated from the goal position. (b) Heading performance by the proposed method. The hit ball successfully tracked the desired trajectory and passed around the goal position. Notably, the monopod also learned to maintain its balance to the hit ball.

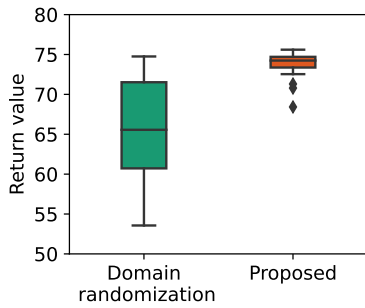


Fig. 5. Multitask heading performance. the domain randomization approach could not achieve a satisfactory multitask performance (green bar). Multiple tasks on multiple environments are successfully accomplished using the proposed method (red bar).

B. Policy selection performance

Herein, we evaluated how the selected policy model based on the proposed method performed better than a randomly selected model. To compare the selection performances, we adopted the top-one regret as the performance measure. Concrete calculation of the top-one regret is described in Section IV-F.

The top-one regret score of the proposed method was 1.4, whereas that of the random selection was 5.1. As the smaller regret showed better performance, we confirmed that the proposed method contributed to select a potentially well-performing policy after the adaptation phase.

C. Adapting to a novel task

In this section, we showed how the adaptation phase of our proposed method modifies a policy to cope with a novel task. We only modulated the one-dimensional latent variable z to improve the task performance for the newly provided task.

The optimization procedure of the latent variable based on the TPE is explained in Section III-C3.

We depicted how the proposed adaptation method improved the task performance in Fig. 6. As shown in Fig. 6(a), the hit ball did not track the desired trajectory and deviated from the goal before the adaptation. To evaluate the task performance before the adaptation, here, we set the latent variable to zero, that is, $z = 0.0$, assuming that we did not have prior knowledge of the novel task before the adaptation. After only 100 trials, the latent variable was successfully optimized such that the modulated policy successfully hit the ball towards the new goal position, as shown in Fig. 6(b).

We also evaluated the overall performances of the policies before and after adaptation on 32 different novel tasks, wherein the tasks were generated randomly, as described in Section IV-E. Fig. 7 shows the task performances of each policy. Before the adaptation, for most novel tasks, task performances were unsatisfactory. Furthermore, performances were varied. After adaptation, the modified policies for novel tasks consistently achieved successful heading performances.

VI. DISCUSSION

A. Adaptation through latent variable optimization

One may consider that the comparison presented in Fig. 5 is not fair because the proposed method conducted additional 100 trials for adaptation. Therefore, we conducted fine-tuning trials on the novel domain to observe how the policy trained by domain randomization can improve with additional 100 learning iterations.

Fig. 8 shows the heading performances with the 32 randomly selected domains. We found that the task performances became worse than those before the fine-tuning trials. This result indicated that the domain randomization policy model could not adapt to new domains with only a small number of additional trials. In other words, extracting the low-

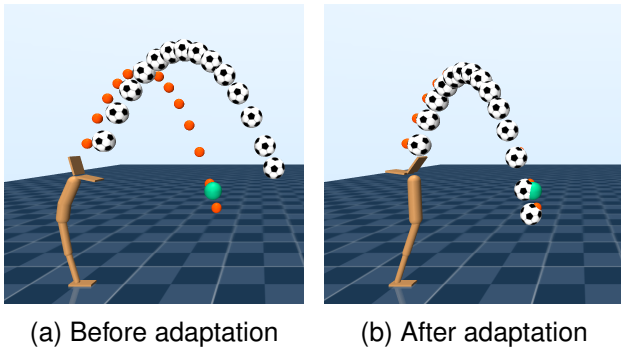


Fig. 6. Heading performance on novel tasks. The green sphere indicates the goal position. The red dot indicates the desired trajectory. (a) Before adaptation: the hit ball did not track the desired trajectory and deviated from the goal. (b) After adaptation: only after 100 adaptation trials, the latent variable was successfully optimized such that the modulated policy successfully hit the ball towards the new goal position.

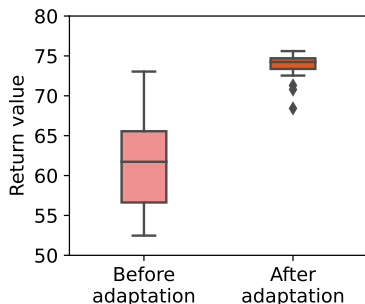


Fig. 7. Multitask heading performances. Before adaptation, task performances were unsatisfactory and varied. After adaptation, modified policies for novel tasks consistently achieved successful heading performances.

dimensional latent space and optimizing the latent variable were significant procedures for adapting a policy to novel tasks and environments.

B. Adaptation through the encoder with explicit context information

In this study, we assumed that the policy could not observe the context variable in the adaptation phase as we usually do not possess information regarding novel domains. However, it would be interesting to investigate how task performance can be improved if the context variable was observable. Here, we explicitly encoded the context variable of 32 novel domains using the trained encoder in the adaptation phase. The outputs of the encoder were forwarded to the policy network as latent variables.

Fig. 9 shows the task performances using explicit context information. Interestingly, the proposed adaptation method showed better heading performances than the method using context information. On the one hand, this is because the context variables for novel domains were not used when the encoder network was trained. On the other hand, even the encoder used in our method was not trained with novel context information. However, our proposed method was able to achieve better performance than the method that considers

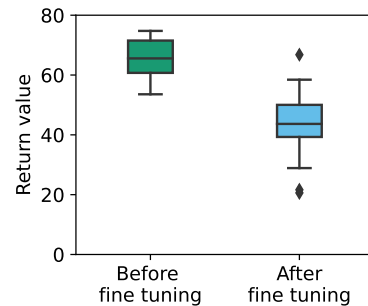


Fig. 8. Fine-tuning performance. We found that task performances became worse than those before fine-tuning trials. This result indicated that the policy modal could not adapt to new domains with only a small number of additional trials.

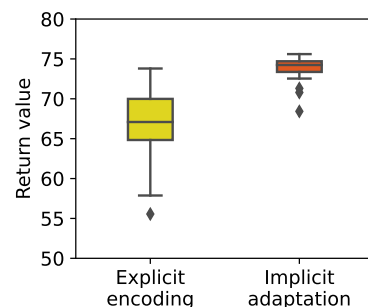


Fig. 9. The proposed method was compared with the baseline method using context variable information. Interestingly, the proposed adaptation method showed a better heading performance than the method using context information. This result empirically showed that we extracted a meaningful latent space for the given movement category.

the context variables as inputs. This result empirically showed that we extracted a meaningful latent space for the given movement category.

VII. CONCLUSION

In this study, we proposed a policy adaptation method for multitask reinforcement learning problems. We particularly focused on dynamic movement tasks in which small changes in the movements lead to completely different consequences. As a concrete task, we consider the multi-heading task by the monopod model. In this task, the monopod learned to hit a ball back to multiple target positions. Furthermore, the coefficient of restitution of the ball also varied. In the adaptation phase of our proposed method, context variables such as goal positions and environmental settings were not provided to the monopod model. Therefore, the learning system needed to adapt to implicitly changed contexts. We showed that the monopod model accomplished 32 different heading tasks after the adaptation process. For the adaptation, we selected one policy among 25 candidate policies based on the return values acquired in the policy generation phase. These policy generation and selection strategies to find adaptable policy models were important factors for successful adaptation.

As we focused on a dynamic movement task that only requires a small change to accomplish different targets in

different environmental settings, we could expect that the latent variable, which represents different contexts, can belong to a low-dimensional space. We empirically found that adapting a one-dimensional latent variable to cope with different situations can be highly effective to achieve higher return values.

As a future study, we aim to explore the possibility of the proposed method on a multi-agent learning problem. We are interested in observing how our proposed method can be utilized to modify agent policy according to implicit changes in other agents' strategies.

ACKNOWLEDGMENTS

This study used several opensource software projects, such as PyTorch [27], rllkit [28], dm-control [29], and Optuna [24]. We are grateful to the project contributors for providing valuable machine learning tools. This work was supported by JSPS KAKENHI (Grant number: 19J22987); by project JPNP20006, commissioned by NEDO; by JST Moonshot R&D program (Grant number: JPMJMS223B-3); and by Tateisi Science and Technology Foundation.

REFERENCES

- [1] L. Zintgraf, K. Shiarli, V. Kurin, K. Hofmann, and S. Whiteson, "Fast Context Adaptation via Meta-Learning," in *Proceedings of the 36th International Conference on Machine Learning*, K. Chaudhuri and R. Salakhutdinov, Eds., vol. 97. Long Beach, California, USA: PMLR, June, 9-15, 2019, pp. 7693–7702.
- [2] A. Nagabandi, I. Clavera, S. Liu, R. S. Fearing, P. Abbeel, S. Levine, and C. Finn, "Learning to Adapt in Dynamic, Real-World Environments through Meta-Reinforcement Learning," in *7th International Conference on Learning Representations*. New Orleans, LA, USA: OpenReview.net, May, 6-9, 2019.
- [3] K. Rakelly, A. Zhou, C. Finn, S. Levine, and D. Quillen, "Efficient Off-Policy Meta-Reinforcement Learning via Probabilistic Context Variables," in *Proceedings of the 36th International Conference on Machine Learning*, K. Chaudhuri and R. Salakhutdinov, Eds., vol. 97. Long Beach, California, USA: PMLR, June, 9-15, 2019, pp. 5331–5340.
- [4] X. B. Peng, E. Coumans, T. Zhang, T.-W. E. Lee, J. Tan, and S. Levine, "Learning Agile Robotic Locomotion Skills by Imitating Animals," in *Proceedings of Robotics: Science and Systems XVI*, Held Virtually, July, 12-16, 2020.
- [5] M. Andrychowicz, F. Wolski, A. Ray, J. Schneider, R. Fong, P. Welinder, B. McGrew, J. Tobin, O. Pieter Abbeel, and W. Zaremba, "Hindsight Experience Replay," in *Advances in Neural Information Processing Systems*, I. Guyon, U. V. Luxburg, S. Bengio, H. Wallach, R. Fergus, S. Vishwanathan, and R. Garnett, Eds., vol. 30. Long Beach, CA, USA: Curran Associates, Inc., Dec, 4-9, 2017, pp. 5048–5058.
- [6] T. Schaul, D. Horgan, K. Gregor, and D. Silver, "Universal Value Function Approximators," in *Proceedings of the 32nd International Conference on Machine Learning*, F. Bach and D. Blei, Eds., vol. 37. Lille, France: PMLR, Jul, 07–09, 2015, pp. 1312–1320.
- [7] M. Liu, M. Zhu, and W. Zhang, "Goal-Conditioned Reinforcement Learning: Problems and Solutions," in *Proceedings of the Thirty-First International Joint Conference on Artificial Intelligence*, L. D. Raedt, Ed. Vienna, Austria: ijcai.org, July, 23-29, 2022, pp. 5502–5511.
- [8] S. Whitehead, J. Karlsson, and J. Tenenber, "Learning Multiple Goal Behavior via Task Decomposition and Dynamic Policy Merging," in *Robot Learning. The Springer International Series in Engineering and Computer Science*, J. H. Connell and S. Mahadevan, Eds. Boston, MA, USA: Springer US, 1993, vol. 233, pp. 45–78.
- [9] S. P. Singh, "Transfer of Learning Across Compositions of Sequential Tasks," in *Proceedings of the Eighth International Workshop (ML91)*, L. A. Birnbaum and G. C. Collins, Eds. Evanston, Illinois, USA: Morgan Kaufmann, 1991, pp. 348–352.
- [10] A. Nair, S. Bahl, A. Khazatsky, V. Pong, G. Berseth, and S. Levine, "Contextual Imagined Goals for Self-Supervised Robotic Learning," in *Proceedings of the 3rd Annual Conference on Robot Learning*, ser. PMLR, L. P. Kaelbling, D. Kragic, and K. Sugiura, Eds., vol. 100. Osaka, Japan: PMLR, Oct. 30, pp. 530–539.
- [11] D. J. Foster and P. Dayan, "Structure in the Space of Value Functions," *Machine Learning*, vol. 49, no. 2-3, pp. 325–346, 2002.
- [12] J.-J. E. Slotine and W. Li, *Applied Nonlinear Control*. Englewood Cliffs, New Jersey, USA: Prentice Hall, 1991.
- [13] J. Morimoto and C. G. Atkeson, "Minimax Differential Dynamic Programming: An Application to Robust Biped Walking," in *Advances in Neural Information Processing Systems*, S. Becker, S. Thrun, and K. Obermayer, Eds., vol. 15. Vancouver, British Columbia, Canada: MIT Press, Dec, 9-14, 2002, pp. 1563–1570.
- [14] J. Morimoto and C. G. Atkeson, "Nonparametric representation of an approximated Poincaré map for learning biped locomotion," *Autonomous Robots*, vol. 27, no. 2, pp. 131–144, 2009.
- [15] W. Yu, J. Tan, C. K. Liu, and G. Turk, "Preparing for the Unknown: Learning a Universal Policy with Online System Identification," in *Proceedings of Robotics: Science and Systems XIII*, N. M. Amato, S. S. Srinivasa, N. Ayanian, and S. Kuindersma, Eds., Cambridge, Massachusetts, USA, July, 12-16, 2017.
- [16] W. Yu, V. C. V. Kumar, G. Turk, and C. K. Liu, "Sim-to-real transfer for biped locomotion," in *2019 IEEE/RSJ International Conference on Intelligent Robots and Systems (IROS)*. Macau, China: IEEE, Nov, 4-8, 2019, pp. 3503–3510.
- [17] C. Gulcehre, Z. Wang, A. Novikov, T. Paine, S. Gómez, K. Zolna, R. Agarwal, J. S. Merel, D. J. Mankowitz, C. Paduraru, G. Dulac-Arnold, J. Li, M. Norouzi, M. Hoffman, N. Heess, and N. de Freitas, "RL Unplugged: A Suite of Benchmarks for Offline Reinforcement Learning," in *Advances in Neural Information Processing Systems*, H. Larochelle, M. Ranzato, R. Hadsell, M. F. Balcan, and H. Lin, Eds., vol. 33. virtual: Curran Associates, Inc., Dec, 6-12, 2020, pp. 7248–7259.
- [18] D. Wierstra, T. Schaul, T. Glasmachers, Y. Sun, J. Peters, and J. Schmidhuber, "Natural Evolution Strategies," *The Journal of Machine Learning Research*, vol. 15, no. 27, pp. 949–980, 2014.
- [19] T. Salimans, J. Ho, X. Chen, S. Sidor, and I. Sutskever, "Evolution Strategies as a Scalable Alternative to Reinforcement Learning," *arXiv e-prints arXiv:1703.03864 [stat.ML]*, Mar. 2017. [Online]. Available: <https://arxiv.org/abs/1703.03864>
- [20] J. Bergstra, R. Bardenet, Y. Bengio, and B. Kégl, "Algorithms for Hyperparameter Optimization," in *Advances in Neural Information Processing Systems*, J. Shawe-Taylor, R. Zemel, P. Bartlett, F. Pereira, and K. Q. Weinberger, Eds., vol. 24. Granada, Spain: Curran Associates, Inc., Dec, 12-17, 2011, pp. 2546–2554.
- [21] J. Bergstra, D. Yamins, and D. Cox, "Making a Science of Model Search: Hyperparameter Optimization in Hundreds of Dimensions for Vision Architectures," in *Proceedings of the 30th International Conference on Machine Learning*, ser. PMLR, S. Dasgupta and D. McAllester, Eds., vol. 28, no. 1. Atlanta, Georgia, USA: PMLR, Jun, 17–19, 2013, pp. 115–123.
- [22] T. Haarnoja, A. Zhou, P. Abbeel, and S. Levine, "Soft Actor-Critic: Off-Policy Maximum Entropy Deep Reinforcement Learning with a Stochastic Actor," in *Proceedings of the 35th International Conference on Machine Learning*, J. Dy and A. Krause, Eds., vol. 80. Stockholm, Sweden: PMLR, July, 10-15, 2018, pp. 1861–1870.
- [23] S. Levine, "Reinforcement Learning and Control as Probabilistic Inference: Tutorial and Review," *arXiv e-prints arXiv:1805.00909 [cs.LG]*, May 2018. [Online]. Available: <http://arxiv.org/abs/1805.00909>
- [24] T. Akiba, S. Sano, T. Yanase, T. Ohta, and M. Koyama, "Optuna: A Next-Generation Hyperparameter Optimization Framework," in *Proceedings of the 25th ACM SIGKDD International Conference on Knowledge Discovery & Data Mining*, A. Teredesai, V. Kumar, Y. Li, R. Rosales, E. Terzi, and G. Karypis, Eds. Anchorage, AK, USA: ACM, Aug, 4-8, 2019, pp. 2623–2631.
- [25] E. Todorov, T. Erez, and Y. Tassa, "MuJoCo: A physics engine for model-based control," in *2012 IEEE/RSJ International Conference on Intelligent Robots and Systems (IROS)*. Vilamoura, Portugal: IEEE, Oct, 7-12, 2012, pp. 5026–5033.
- [26] J. Fu, M. Norouzi, O. Nachum, G. Tucker, Z. Wang, A. Novikov, M. Yang, M. R. Zhang, Y. Chen, A. Kumar, C. Paduraru, S. Levine, and T. Paine, "Benchmarks for Deep Off-Policy Evaluation," in *9th International Conference on Learning Representations*. Virtual Event, Austria: OpenReview.net, May, 3-7, 2021.
- [27] A. Paszke, S. Gross, F. Massa, A. Lerer, J. Bradbury, G. Chanan, R. Killeen, Z. Lin, N. Gimelshein, L. Antiga, A. Desmaison, A. Kopf, E. Yang, Z. DeVito, M. Raison, A. Tejani, S. Chilamkurthy, B. Steiner, L. Fang, J. Bai, and S. Chintala, "PyTorch: An Imperative Style, High-Performance Deep Learning Library," in *Advances in Neural Information Processing Systems*, H. Wallach, H. Larochelle, A. Beygelzimer, F. D'

- Alché-Buc, E. Fox, and R. Garnett, Eds., vol. 32. Vancouver, BC, Canada: Curran Associates, Inc., Dec, 8-14, 2019, pp. 8024–8035.
- [28] V. Pong, A. Nair, M. Dalal, and S. Lin, “RLkit.” [Online]. Available: <https://github.com/rail-berkeley/rlkit>
- [29] S. Tunyasuvunakool, A. Muldal, Y. Doron, S. Liu, S. Bohez, J. Merel, T. Erez, T. Lillicrap, N. Heess, and Y. Tassa, “Dm_control: Software and Tasks for Continuous Control,” *Software Impacts*, vol. 6, p. 100022, 2020.
- [30] S. Fujimoto, H. van Hoof, and D. Meger, “Addressing Function Approximation Error in Actor-Critic Methods,” in *Proceedings of the 35th International Conference on Machine Learning*, J. Dy and A. Krause, Eds., vol. 80. Stockholm, Sweden: PMLR, July, 10-15, 2018, pp. 1587–1596.
- [31] V. Mnih, K. Kavukcuoglu, D. Silver, A. A. Rusu, J. Veness, M. G. Bellemare, A. Graves, M. Riedmiller, A. K. Fidjeland, G. Ostrovski, S. Petersen, C. Beattie, A. Sadik, I. Antonoglou, H. King, D. Kumaran, D. Wierstra, S. Legg, and D. Hassabis, “Human-level control through deep reinforcement learning,” *Nature*, vol. 518, no. 7540, pp. 529–533, 2015.
- [32] T. P. Lillicrap, J. J. Hunt, A. Pritzel, N. Heess, T. Erez, Y. Tassa, D. Silver, and D. Wierstra, “Continuous control with deep reinforcement learning,” in *4th International Conference on Learning Representations*, Y. Bengio and Y. LeCun, Eds., San Juan, Puerto Rico, May, 2-4, 2016.
- [33] T. Haarnoja, A. Zhou, K. Hartikainen, G. Tucker, S. Ha, J. Tan, V. Kumar, H. Zhu, A. Gupta, P. Abbeel, and S. Levine, “Soft Actor-Critic Algorithms and Applications,” *arXiv e-prints arXiv:1812.05905 [cs.LG]*, Dec. 2018. [Online]. Available: <http://arxiv.org/abs/1812.05905>

APPENDIX

A. Learning algorithm

We adopted the target networks, clipped double- Q learning, and entropy autotuning in the policy generation phase. The target network and clipped double- Q learning are the methods used for reducing the estimation error of Q functions. For this purpose, four neural networks were trained to approximate a single Q function. Entropy autotuning changes the temperature parameter α that controls the exploration and exploitation trade-off.

1) *Clipped double- Q learning*: Q -function networks were trained to reduce Bellman residuals, as shown in Eq. (17) as follows:

$$\begin{aligned} \min_{\phi_i} \mathbb{E}_{\mathcal{D}} \left(Q(s, a, c; \phi_i) - r(s, a, c) - \gamma \bar{V}(s', c) \right)^2, \quad (17) \\ \bar{V}(s, c) := \min_{i \in \{1, 2\}} Q(s, a', c; \phi_i^{\text{target}}) - \alpha \log \pi(a' | s, z; \psi), \\ a' \sim \pi(a' | s, z; \psi), z \sim q(z | c; \eta), \{s, a, s', c\} \sim \mathcal{D}, \end{aligned}$$

where ϕ_i and ϕ_{target} are the Q -network parameters; r , γ , and α denote the reward function, discount factor, and temperature parameter, respectively; π represents the policy; q represents the encoder; and \mathcal{D} is the state-action pair data stored in a replay buffer. The value function \bar{V} was computed from $Q(s', a', c)$, where s' , a' and c are the state, action, and context at the next step, respectively. Simply using the above method tends to overestimate the action values; therefor, clipped double- Q Learning was proposed to overcome this overestimation problem [30]. To use this method, we trained two networks and selected the smaller output of the two approximated Q functions to derive the value \bar{V} . In practice, Q values at the next step are derived from the target network ϕ_{target} explained below.

2) *Target networks*: The target networks were used to stabilize the learning process of the Q function. As we explained in the previous section, the target value V was derived from the Q network, which caused the target value estimation to be unstable [31]. Therefore, as suggested in [32], we updated the target network through moving average as follows:

$$\phi_i^{\text{target}} \leftarrow \tau \phi_i + (1 - \tau) \phi_i^{\text{target}}. \quad (18)$$

The Polyak’s coefficient τ , which ranges from 0 to 1, was used to adjust the update rate.

3) *Entropy autotuning*: To autotune the temperature parameter α of the entropy regularization term, we considered the following optimization problem [33]: H is the conditional entropy of the policy distribution given the state s , and \bar{H} is the target entropy set by an experimenter. The target entropy was set to -1 times the action dimension $|A|$ as follow [33]:

$$\max_{\pi} \mathbb{E}_{\tau \sim \mathcal{D}} \left[\sum_t \gamma^t r_t \right], \quad (19)$$

$$\text{s.t. } \mathbb{E}_{s \sim \mathcal{D}} [H(\pi)] < \bar{H}. \quad (20)$$

Although this equation does not explicitly contain the temperature parameter α , it can be attributed to the following min-max problem as Lagrange duality when the temperature parameter α is regarded as a Lagrange multiplier:

$$\min_{\alpha > 0} \max_{\pi} \mathbb{E}_{\tau \sim \mathcal{D}} \left[\sum_t \gamma^t r_t - \alpha (\log \pi_t + \bar{H}) \right]. \quad (21)$$

The min-max problem was solved as:

$$\min_{\alpha > 0} \mathbb{E}_{(a, s, z) \sim \mathcal{D}} \left[\alpha (-\log \pi(a | s, z) - \bar{H}) \right]. \quad (22)$$

A heuristic transformation $\alpha \leftarrow \exp(\alpha)$ was performed on the temperature parameter α to guarantee the positive value as practical implementation¹.

B. Policy gradient and reparametrization trick

We used the reparametrization trick to calculate the gradient of the objective function with respect to policy parameters. The objective function was expressed as follows:

$$\begin{aligned} \max_{\psi, \eta} \mathbb{E}_{(s, c) \sim \mathcal{D}} [\bar{V}(s, c)] - \beta \mathbb{E}_{c \sim \mathcal{D}} \text{KL} [q || \rho], \quad (23) \\ a' \sim \pi(a' | s, z; \psi), z \sim q(z | c; \eta), \rho(z) = \mathcal{N}(z | \mathbf{0}, \sigma \mathbf{I}). \end{aligned}$$

Here, ϕ and η are the network parameters of the policy π and encoder q networks, respectively; and $\rho(z)$ is the prior distribution of the latent variable.

To derive the gradient, expectation over the policy distribution π and encoder distribution q must be evaluated as follows:

$$\begin{aligned} \max_{\psi, \eta} \mathbb{E}_{(s, c) \sim \mathcal{D}, q \pi} [Q(s, a, c) - \alpha \log \pi(a | s, z; \psi)] \\ - \beta \mathbb{E}_{c \sim \mathcal{D}, q} \left[\log \frac{q(z | c; \eta)}{\rho(z)} \right]. \quad (24) \end{aligned}$$

¹<https://github.com/rail-berkeley/softlearning/blob/master/softlearning/algorithms/sac.py#L140>. Accessed: July-10, 2023

By defining the related variables as shown below, the parameters of the neural network do not depend directly on the distributions.

$$a = \tanh(f(s, z; \psi) + \sigma(s, z; \psi)\epsilon), \epsilon \sim \mathcal{N}(\mathbf{0}, \mathbf{I}), \quad (25)$$

$$z = g(c; \eta) + \delta\omega, \omega \sim \mathcal{N}(\mathbf{0}, \mathbf{I}), \quad (26)$$

$$P(a; \psi) = P(\epsilon) \left| \frac{da}{d\epsilon} \right|_{\psi}^{-1}, P(z; \eta) = P(\omega) \left| \frac{dz}{d\omega} \right|_{\eta}^{-1}. \quad (27)$$

Here, ϵ and ω are the random variables sampled from the standard normal distribution; and f , σ , and g are the functions represented by the neural networks. Now, the objective function can be defined as,

$$\begin{aligned} J(\psi, \eta) = & \mathbb{E}_{(s,c) \sim \mathcal{D}, \omega, \epsilon} [Q(s, a, c) - \alpha \log \pi(a|s, z; \psi)] \\ & - \beta \mathbb{E}_{c \sim \mathcal{D}, \omega} \left[\log \frac{q(z|c; \eta)}{\rho(z)} \right], \\ & a = a(s, \epsilon, z; \psi), z = z(c, \omega; \eta), \end{aligned}$$

where the integrated variables, ϵ and ω , are independent of the network parameters. Therefore, the interchange of the gradient and integral for the policy and encoder parameters, ψ and η , was allowed:

$$\begin{aligned} \nabla J &= \nabla \mathbb{E}_{(s,c) \sim \mathcal{D}, \omega, \epsilon} \left[Q - \alpha \log \pi - \beta \log \frac{q}{\rho} \right], \\ &= \mathbb{E}_{(s,c) \sim \mathcal{D}, \omega, \epsilon} \left[\nabla Q - \alpha \nabla \log \pi - \beta \nabla \log \frac{q}{\rho} \right]. \quad (28) \end{aligned}$$

C. Hyperparameters

The parameters used in this study are listed in Table III. Notably, most of the parameters were selected based on those reported in the study by Haarnoja et al. [33].

TABLE III
LIST OF HYPERPARAMETERS

hyperparameter	policy search	adaptation
action time period	25ms	25 ms
neural network optimizer	Adam	Adam
Policy and encoder learning rate	3×10^{-4}	-
Q learning rate	0.001	-
β	e^{-5}	e^{-5}
replay buffer size	10^6	100
collect step size per training	1000	100
collect step size per evaluation	1000	100
update times per training	1000	10
Polyak's coefficient τ	0.01	-
batch size	256	100
discount γ	0.99	1.00
optimization algorithm	Adam	Adam
encoder variance δ	0.01	0.01
prior variance σ	1	1
target entropy	$- \mathcal{A} $	-
temperature α	-	0.01
k_{\max}	-	100